

Nonparabolic behavior of GaSb-AlSb quantum wells under hydrostatic pressure

P. Lefebvre, B. Gil, J. Allegre, H. Mathieu, and Y. Chen

*Groupe d'Etude des Semiconducteurs, Université des Sciences et Techniques du Languedoc,
Place Eugène Bataillon, 34060 Montpellier Cedex, France*

C. Raisin

*Laboratoire d'Etude des Surfaces, Interfaces et Composants, Université des Sciences et Techniques du Languedoc,
Place Eugène Bataillon, 34060 Montpellier Cedex, France*

(Received 9 July 1986)

We present a photoluminescence investigation of the electronic properties of a strained GaSb-AlSb quantum well under hydrostatic pressure. Our experiment, performed at liquid-helium temperature, permits us to measure a pressure shift of the quantized exciton smaller than the GaSb band-gap shift. Such an effect is analyzed in the framework of a model calculation which takes account of the nonparabolicity and of the change of the quantized Rydberg (R^*) versus pressure. We find $1/R^*(dR^*/dP) \sim 1\%/kbar$. We estimate a valence-band offset $\Delta E_v \sim 40$ meV.

I. INTRODUCTION

The GaSb-AlSb quantum-well structure (QW) is a strained type-I quantum well: first, both electrons and holes are confined in the GaSb layer; and second, the accommodation of the lattice mismatch by elastic deformation induces a shrinkage of the GaSb band gap and a splitting of the Γ_8 valence band.

In this paper, we report photoluminescence experiments performed at low temperature and under hydrostatic pressure on GaSb-AlSb QW grown by molecular-beam epitaxy (MBE). In order to discuss the behavior of the transitions observed in optical experiments, different phenomena have to be taken into account: (i) biaxial strain effects, (ii) excitonic and nonparabolicity effects, and (iii) hydrostatic pressure effects.

The accommodation of the lattice mismatch by elastic strain induces changes in electronic properties which are quantitatively comparable to the quantum size effect ones. Moreover, depending on the thickness of the GaSb layer, the difference between the confinement energy and the valence-band splitting may induce a reversal of the energy position of the heavy- and light-hole subbands. This point has clearly been discussed in a series of papers by Voisin *et al.*^{1,2}

Concerning the excitonic character of the optical transition, it is worth noting that in a type-I QW, the exciton binding energy is always larger than the three-dimensional (3D) Rydberg. It varies continuously with the well thickness from the two-dimensional case ($L_z \sim 0$) toward the three-dimensional one ($L_z \gg a_\infty$, where a_∞ is the Bohr radius of the transversal exciton).³⁻⁵ Moreover, the nonparabolicity effect cannot be ignored, first because GaSb has a nonparabolic band structure and second because it will contribute significantly as soon as the well thickness is smaller than the effective Bohr radius of the carrier under investigation. The influence of the nonparabolicity effect has been shown to be important in GaAs-Ga_{1-x}Al_xAs QW.⁶

Lastly, the band gap widens with hydrostatic pressure and leads to strong variations of the electron and hole effective masses. This leads to a pressure dependence of both the electron and hole confinement energies and of the excitonic binding energy.

The paper is organized as follows. First we detail the experimental procedure and the luminescence patterns collected up to 7 kbar at 2 K. Then, we give the basic ingredients for the theoretical treatment and lastly we compare experiment and calculation.

II. EXPERIMENTAL DETAILS

Our sample was grown on a [001] oriented GaSb substrate by (MBE) with the following sequence: a 1000-Å-thick AlSb buffer, a (78 ± 3) -Å GaSb layer, then 200 Å of AlSb, and finally a 100-Å GaSb passivation layer. Details have been given elsewhere.⁷ The hydrostatic pressure cell was a conventional one built by Unipress-Warsaw, made of copper beryllium, and fitted with an optical sapphire window. At room temperature, the device was charged with a transparent pressure-transmitting medium and compressed to a maximum value of about 11 kbar. After cooling down to liquid-helium temperature, an indium antimonide pressure gauge was used to calibrate the pressure.⁸ A maximum value of 7 kbar could be reached. Changing the pressure required warming up the system to 300 K and then cooling down again. The luminescence was pumped using a typical power of 100 mW with the 647-nm line of an ionized krypton laser and detected with a PbS detector and a 75-cm focal length Jobin-Yvon spectrometer.

III. EXPERIMENTAL RESULTS

Two contributions must be selected in the luminescence spectra which are given in Fig. 1 for several pressures: (i) First, we observe the well-known transitions $e-A_0$ (778 meV at 2 K and $P=0$) and A_0X (796 meV at 2 K and $P=0$);⁹ both are characteristic of the bulk p -type GaSb

substrate. The prevailing transition ($e-A_0$) corresponds to the band-acceptor transition involving nonstoichiometric residual defects.^{10,11} A_0X corresponds to the recombination of an exciton bound to this acceptor; the A_0X intensity noticeably increases as soon as the carrier concentration decreases to around a few 10^{16} cm^{-3} . Both A_0X and $e-A_0$ permit us to follow the pressure dependence of the GaSb Γ_{8v} - Γ_{6c} band gap. (ii) Second, a broad luminescence peak (half-height width ~ 15 meV) characteristic of the QW appears above the GaSb band gap at 838 meV in pumped liquid helium and under atmospheric pressure conditions. This excessive width is characteristic of excitons in QW of low quality and may be interpreted in terms of exciton trapping on interface defects¹²⁻¹⁴ of typically 300 Å diameter and 2 monolayers depth. Bastard *et al.*¹² have shown that the binding energy of the exciton to these planar defects can reach 5 meV for GaAs-Ga_{1-x}Al_xAs QW. We have estimated the broadening of the luminescence peak in the framework of these ideas and found a value of typically 10 meV when the mean

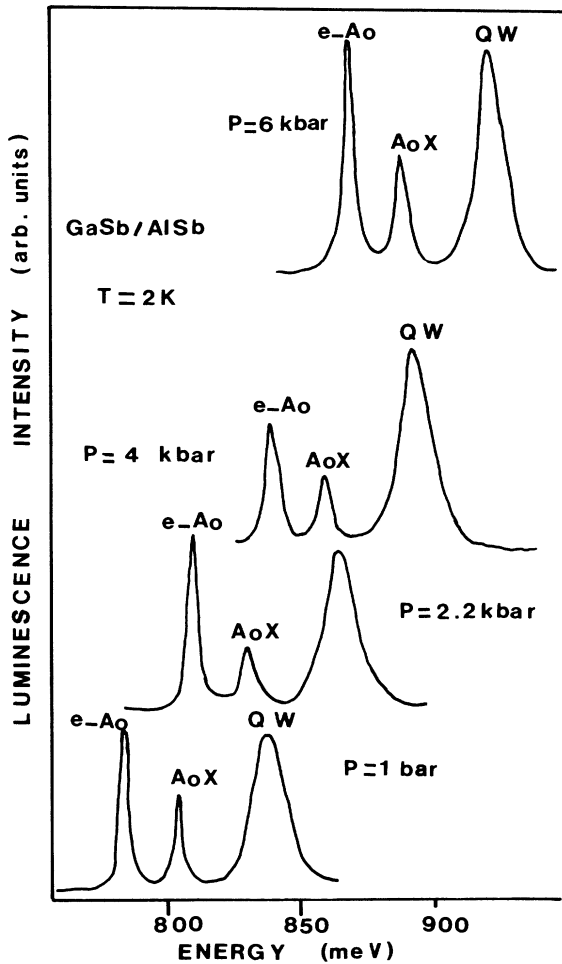


FIG. 1. Pressure dependence of the luminescence spectrum. QW represents the electron-light-hole optically active recombination of the carriers in the quantum well. Both $e-A_0$ and A_0X correspond to the GaSb substrate.

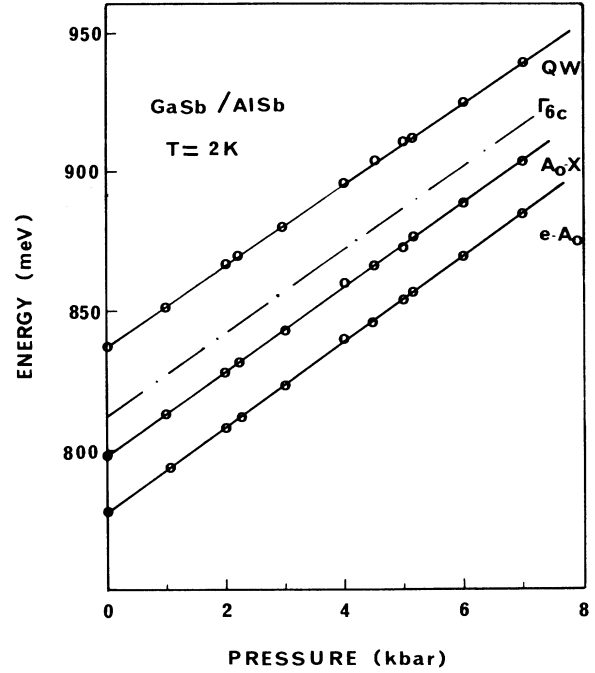


FIG. 2. Pressure shift of the three luminescence lines. The pressure shift of QW is $94 \pm 1\%$ of the GaSb band gap.

depth of these defects is one monolayer and ~ 13 meV when the depth reaches 2 monolayers. This is, roughly speaking, in agreement with our experimental finding.

The pressure shifts of the three luminescence bands discussed above are gathered in Fig. 2. The pressure coefficients have been obtained from a least-mean-squares fit of the experimental data. The pressure coefficient of the QW luminescence line is *smaller* and equals $94 \pm 1\%$ of the pressure coefficient of the $e-A_0$ and A_0X transitions. As we shall see in Sec. V, this is a typical effect of nonparabolicity.

IV. CALCULATION OF THE ELECTRONIC STATES

A. Lattice mismatch effects

Our sample has been grown on a *thick* AISb buffer which presents a mismatch with the GaSb substrate but relaxes to its own lattice parameter. The thick AISb buffer emphasizes its lattice constant to the thin sandwiched GaSb layer which experiences a biaxial stretching along both the x and y directions. The resulting structural crystallographic ordering of the atoms in the heterostructure can be obtained according to the ideas developed by Voisin¹ and Voisin *et al.*²

Let a_{\perp} be the interfacial lattice parameter of the strained layer and a_i ($i=1,2$) be the unstrained lattice parameter of both materials in contact. The nonvanishing strains are $e_{xx}^i = e_{yy}^i = (a_{\perp} - a_i)/a_i$ and $e_{zz}^i = (a_z^i - a_i)/a_i$. The elementary elasticity theory gives the stress-strain relation. The magnitude of the corresponding stress is

$$X_i = 1/S_i(a_{\perp} - a_i)/a_i$$

with

$$S_i = (S_{11} + S_{12})i.$$

In order to calculate the a_{\perp} interfacial parameter we have to minimize the total free energy of the structure:

$$E = \sum_i E_i = \sum_{(vi)} (a_{\perp} - a_i)/a_i d\tau/S_i$$

with respect to a_{\perp} . The QW has $D_{2d}^{(001)}$ orientational symmetry with a fourfold axis lying along the $\langle 001 \rangle$ growth axis. As a consequence of such a lowering of cubic symmetry, the GaSb valence-band states will not remain degenerate at $k=0$. The GaSb valence-band splitting can be calculated following the standard method¹⁵ and extensively applied for specific problems of III-V compounds.^{16,17} Table I summarizes the values of the physical quantities that are of interest for a numerical investigation of the experimental data shown above. The tensile stress X_I gives a $2b(S_{11} - S_{12})X_I$ splitting of $|3/2 \pm 1/2\rangle$ and $|3/2 \pm 3/2\rangle$ Γ_8 related hole states. The shrinkage of the GaSb band gap leads to a situation where the valence-band ground state should be $|3/2 \pm 1/2\rangle$. Of course, the stress-induced coupling with Γ_7 has been neglected as usual since the spin-orbit coupling is large compared to the stress splitting. We can calculate the QW eigenenergies at the Γ point within the envelope-function formalism of Bastard,¹⁸ using for the light holes and conduction states the modified values of the band gap. We assume both a conduction-band offset ΔE_C and a valence band one ΔE_v between GaSb and AlSb without interfacial stress. The potential depths for light holes (LH) and heavy holes (HH) are, respectively,²

$$\Delta E_v^{LH} = \Delta E_v - b(S_{11} - S_{12})X_I + 2a(S_{11} + 2S_{12})X_I/3$$

and

TABLE I. Physical constants of GaSb and AlSb.

	GaSb	AlSb
S_{11} (10^{-6} bar $^{-1}$)	1.48 ^a	1.634 ^a
S_{12} (10^{-6} bar $^{-1}$)	-0.45 ^a	-0.552 ^a
S_{44} (10^{-6} bar $^{-1}$)	2.23 ^a	2.38 ^a
Lattice parameter (10^{-10} m)	6.0959 ^b	6.1355 ^b
a (eV)	-8.30	-5.90
b (eV)	-2	-1.35
$\partial E_G/\partial P$ (meV/kbar)	15 ^c	10 ^c
m_0^*e/m_0	0.041 ^b	0.110 ^b
γ_1	11.8 ^d	4.15 ^d
γ_2	4.03 ^d	1.01 ^d
γ_3	5.26 ^d	1.75 ^d

^aReference 28.

^bReference 27.

^cReference 29.

^dReference 26.

$$\Delta E_v^{HH} = \Delta E_v + b(S_{11} - S_{12})X_I + 2a(S_{11} + 2S_{12})X_I/3.$$

For clarity, in order to summarize our notations, we give in Fig. 3 a simple arbitrary real-space representation of the QW, both without pressure and under 6 kbar. In order to simplify that picture, we have drawn only the situation obtained when considering the light holes; the heavy holes have been omitted. Following the notations of Ref. 2, the valence-band offsets of the QW will be noted ΔE_v^{LH} and ΔE_v^{HH} for light holes and heavy holes, respectively. The electron/light-hole binding energies E_e/E_{lh} are measured from the extrema of the conduction/lowest valence band, respectively. $C = \partial E_g/\partial P$ represents the pressure coefficient of the GaSb band gap.

B. Nonparabolicity

The square-well model permits us to calculate the binding energy for both holes and electrons, but we have to take into account the nonparabolicity of the band structure because both the GaSb band gap and the spin-orbit coupling are comparable. In that calculation we have used Kane's three-band model.

The effective mass of the electron will vary as follows:

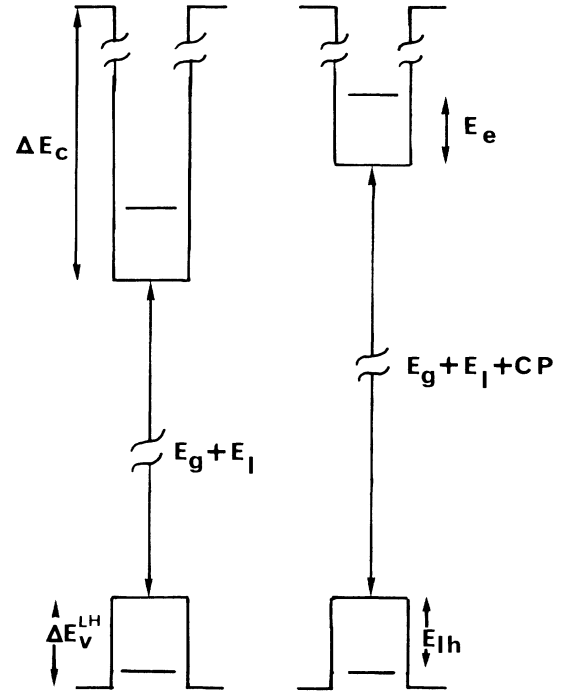


FIG. 3. Schematic picture for the QW at two pressures. The notations are following: ΔE_C (ΔE_v^{LH}) represents the conduction-band (light-hole valence-band) offset; E_g and E_I represent the bulk GaSb band gap and the band gap shrinkage related to the lattice mismatch effect. Both E_e and E_{lh} , the electron and hole confinement energies are measured with respect to the bottom of the conduction band and to the top of the light-hole valence band, respectively. C represents the pressure shift of the direct band gap. The heavy holes have been omitted for the simplicity of that picture.

$$\frac{m_e^*}{m_{0e}^*} = \frac{E_g + E_I + E_e + \Delta + CP + E_h}{E_g + \Delta} \frac{E_g + E_I + E_e + CP + E_h}{E_g} \frac{2E_g + 3\Delta}{2E_h + 2E_g + 2E_I + 2E_e + 3\Delta + 2CP}$$

m_{0e}^* is the bulk GaSb effective mass, E_g is the GaSb band gap (813 meV), E_I is the interfacial contribution, and E_e (E_h) the electron (hole) binding energy. The pressure dependence of the GaSb band gap $C = 15 \text{ meV kbar}^{-1}$ has been measured from the shifts of A_0 and A_0X luminescence lines. It is worth noting that the effective mass is increased by about 2% per kilobar.

The hole effective masses are expressed as a function of the Luttinger parameters according to Altarelli¹⁹ and Marzin:²⁰

$$\frac{m_h^*}{m_{0h}} = \frac{E_g + E_I + CP + E_e + E_h}{E_g + E_I},$$

where m_{0h} is the effective mass for the strained GaSb layer.

C. Excitonic corrections

The electron-hole long-range electrostatic interaction presents a strong well-thickness dependence in the small thickness range.³ As it has been pointed out in Ref. 3, in the case of type-I QW, the exciton motion is close to the two-dimensional limit as soon as the well thickness is typically a third of the 3D Bohr radius.

Each pressure corresponds to a special situation on the dimensionless curve given in Fig. 2 in Ref. 3: Bohr radius, effective mass, and dielectric constant change versus pressure. The exciton binding can be quantitatively calculated for each pressure in the peculiar case of our GaSb-AISb quantum well.

The relative change in the dielectric constant is one order of magnitude smaller than the mass ones.²¹ However, it contributes significantly to the pressure dependence of the 3D Rydberg²² and to the 2D one. In accordance with Camphausen *et al.*,²³ we will take $(1/\epsilon)(d\epsilon/dP) = -0.4 \times 10^{-3} \text{ kbar}^{-1}$.

V. COMPARISON WITH EXPERIMENTS

A. Band-structure scheme

We first calculate the interfacial stress from the equation given in the preceding section. The AISb buffer is 1000 Å thick and the GaSb confining layer has been grown to 78 Å thick. This allows us to calculate the interfacial tensile stress which equals 5.8 kbar. Then we deduce the splitting of the valence-band states: 45.2 meV. Adding the hydrostatic contribution of the interfacial stress we find a band-gap shrinkage from 813 to 735 meV for the $|3/2 \pm 1/2\rangle$ -conduction-band (CB) band gap and 779 meV for the $|3/2 \pm 3/2\rangle$ -CB one. Then the QW is modeled as usual by two potential square wells: one with a depth ΔE_c for the electrons and another with a depth $\Delta E_v + 78 \text{ meV}$ for the light holes. Concerning the heavy holes, the potential depth should be $\Delta E_v + 33 \text{ meV}$. ΔE_c

and ΔE_v are two adjustable parameters which will be deduced after a fitting procedure of our experimental data. The previously reported values of ΔE_v vary from $\sim 50 \text{ meV}$ (Ref. 24) up to 230 meV (Ref. 25). According to the common anion rule the valence-band offset ΔE_v should be small with respect to ΔE_c . Next, the mathematical treatment of that problem requires the effective mass of all particles. The GaSb layer valence band has been described with the standard effective mass for strained QW:²⁰

$$m_z^{1/2} = 1/(\gamma_1 + 2\gamma_2) = 0.05$$

and

$$m_z^{3/2} = 1/(\gamma_1 - 2\gamma_2) = 0.267.$$

These masses do vary nonparabolically. The AISb-hole effective mass has been obtained from the values of the Luttinger parameters given by Lawaetz.²⁶ Concerning the electron mass, we take a parabolic law for AISb ($m_{0e}^* = 0.11m_0$) and a nonparabolic one for GaSb ($m_{0e}^* = 0.042m_0$ for bulk GaSb). We have all the basic ingredients (dielectric constant, masses, QW width) in order to estimate the excitonic Rydberg in the QW. We find a value about 2.45 times the 3D Rydberg, i.e., about 6 meV.

We have fitted ΔE_c and ΔE_v in order to agree with a transition of 838 meV for the confined exciton. We have found a valence-band potential depth of 93 meV for the light hole, to which a zero-strain valence-band offset ΔE_v of 15 meV and a conduction-band potential depth of 1437 meV correspond. In order to check these values, we have repeated our calculation with a smaller QW width (75 Å). However, we could find a set of ΔE_c and ΔE_v which permits us to predict the proper energy transition; this finding does not agree with the experimental data of Voisin *et al.*²⁷ The heavy hole would give a type-II QW; this is not convenient, with the cross section of the optical transition seen in absorption and previously reported by Voisin *et al.*²⁷ The corresponding cross section cannot be understood if both electrons and holes are confined to different parts of the sample. Next, we have fitted a 81-Å-wide GaSb-AISb QW. The value of the valence-band offset necessary to give a quantized transition at 838 meV is then 64 meV and can be compared with the value corresponding to the 78-Å-wide QW (15 meV). Both ΔE_v and ΔE_c are fitted in order to agree with the data at atmospheric pressure and for the entire range of pressure of that work. Given a transition energy, our method leads us to a couple of values which are sensitive to the well width. Since the experimental growth conditions do not allow a knowledge of the GaSb layer width with an accuracy better than 3 Å, we propose to keep the mean value of $40 \pm 25 \text{ meV}$ for ΔE_v ; such a value should be compared with the value of $90 \pm 12 \text{ meV}$ given recently for GaAs-Ga_{1-x}Al_xAs.³⁰ According to the common anion rule, since most of the zone-center valence-band states come

from the $4P$ Sb electronic states, a small value of 40 meV appears to be a very reasonable one.

B. Pressure dependence

We have calculated the pressure dependence of the transition up to 7 kbar. The band gap widens with pressure and leads to strong variations of the effective mass as stated above; this gives a significant contribution to the change of the confinement energy versus pressure. We have plotted in Fig. 4 the experimental shifts of the QW transition with respect to the bulk GaSb band gap. The A_0X and A_0 transitions follow the band gap within the experimental uncertainty but clearly the QW transition does not. Similar experimental findings have also been found in the case of the GaAs-Ga $_{1-x}$ Al $_x$ As multiple quantum well³⁰ and superlattice.³¹ Superimposed on these data, our calculation (solid line) nicely fits the experimental results.

Three contributions to the pressure dependence of the QW transition can be selected: first, the change in electron confinement; second, the change in hole confinement; and third, the change of the excitonic binding versus pressure. We have plotted the results of the calculation concerning these three quantities in Figs. 5(a), 5(b), and 5(c). The change in the electron confinement versus pressure [Fig. 5(a)] is one order of magnitude larger than that of the hole [Fig. 5(b)]; this is not surprising when comparing both ΔE_c and ΔE_v . Most of the contribution to the pressure dependence of the QW transition arises from the electronic part if the change in exciton binding versus pressure is small. This third quantity has been plotted in Fig. 5(c). The Rydberg in the QW presents a small varia-

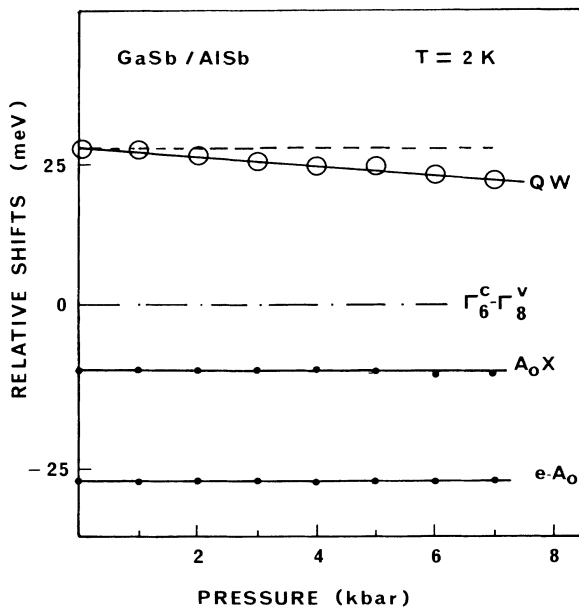


FIG. 4. Relative shift of the three recombination lines versus pressure. The solid lines correspond to the results of our calculation; the dashed one to the previsions of the parabolic model.

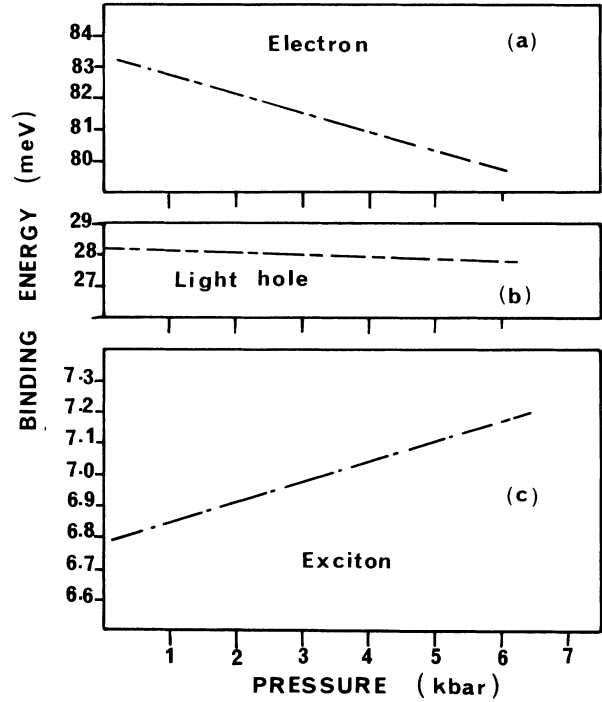


FIG. 5. Different contributions of the pressure dependence of the optical transition related to the QW. (a) Change in electron confinement versus pressure, (b) the same as (a) but for the light hole, and (c) variation of the effective Rydberg in the QW under pressure.

tion versus pressure. We find $(1/R^*)(dR^*/dP) \sim 1\%$ per kbar, which is comparable with the results previously reported in the case of III-V compounds.²²

VI. CONCLUSION

We have measured the hydrostatic pressure dependence of the low-temperature photoluminescence line associated with transitions between the quantized energy levels of a 78-Å-wide GaSb-AlSb quantum well. Resulting from the strain splitting of the Γ_8 valence band and despite the fact that the confinement energy of the light hole is much larger than that of the heavy hole, the ground valence state of the QW is the first light-hole subband LH_1 .

The pressure coefficient of the fundamental QW luminescence line associated with the E_1 - LH_1 transition does not equal the GaSb band-gap one. Analyzing this result in terms of the pressure-induced nonparabolic effect, we show that the most important contribution to the difference arises from the pressure dependence of the electron confinement energy associated with the increase of the electron effective mass under pressure. The relative increase of the exciton binding energy is $\sim 1\%$ per kbar, which is a value generally found for bulk III-V compounds. The valence-band offset is believed to be close to 40 meV, in agreement with the common anion rule.

ACKNOWLEDGMENTS

The Groupe d'Etude des Semiconducteurs and the Laboratoire d'Etude des Surfaces, Interfaces et Composants are "Laboratoires Associés au Centre National de la Recherche Scientifique."

-
- ¹P. Voisin, *Surf. Sci.* **168**, 546 (1986).
²P. Voisin, C. Delalande, G. Bastard, M. Voos, L. L. Chang, A. Segmuller, C. A. Chang, and L. Esaki, *Superlattices Microstructures* **1**, 155 (1985).
³G. Bastard, E. E. Mendez, L. L. Chang, and L. Esaki, *Phys. Rev. B* **26**, 1974 (1982).
⁴Y. Shinozuka and M. Matsuura, *Phys. Rev. B* **28**, 4878 (1983); **29**, 3717 (1984).
⁵R. C. Miller, D. A. Kleinman, W. T. Tsang, and A. C. Gosard, *Phys. Rev. B* **24**, 1134 (1981).
⁶S. Chaudhuri and K. K. Bajaj, *Phys. Rev. B* **29**, 1803 (1984).
⁷C. Raisin, B. Saguintaah, H. Tegmousse, L. Lassabatere, B. Girault, and C. Alibert, *Ann. Telecommun.* **41**, 50 (1986).
⁸N. Konczykowski, M. Baj, E. Szafarkiewicz, L. Konczewicz, and S. Porowski, *High Pressure and Low Temperature Physics* (Plenum, New York, 1978), p. 537.
⁹E. J. Johnson, I. Filinski, and H. Y. Fan, in *Proceedings of the Sixth International Conference on the Physics of Semiconductors, Kyoto, 1962* (unpublished), p. 375.
¹⁰C. Benoit a la Guillaume and P. Lavallard, *Phys. Rev. B* **5**, 490 (1972).
¹¹W. J. Jakowetz, W. Rühle, K. Breuninger, and M. Pilkuhn, *Phys. Status Solidi A* **12**, 169 (1972).
¹²G. Bastard, C. Delalande, M. H. Meynadier, P. M. Frijlink, and M. Voos, *Phys. Rev. B* **29**, 7042 (1984).
¹³C. Delalande, M. H. Meynadier, and M. Voos, *Phys. Rev. B* **31**, 2497 (1985).
¹⁴M. H. Meynadier, C. Delalande, G. Bastard, M. Voos, F. Alexandre, and J. L. Lievin, *Phys. Rev. B* **31**, 5539 (1985).
¹⁵G. L. Bir and G. E. Pikus, *Symmetry and Strained Induced Effects in Semiconductors* (Wiley, New York, 1974).
¹⁶H. Mathieu, J. Camassel, and F. Benckroun, *Phys. Rev. B* **29**, 3438 (1984).
¹⁷B. Gil, J. Camassel, J. P. Albert, and H. Mathieu, *Phys. Rev. B* **33**, 2690 (1986).
¹⁸G. Bastard, *Phys. Rev. B* **24**, 5693 (1981).
¹⁹M. Altarelli, *Phys. Rev. B* **28**, 842 (1983); also see M. Altarelli and U. Ekenberg, *ibid.* **32**, 5138 (1985).
²⁰J. Y. Marzin (unpublished).
²¹G. A. Samara, *Phys. Rev. B* **27**, 3494 (1983).
²²Y. Chen, B. Gil, A. Kadri, J. Allegre, J. Camassel, and H. Mathieu, X AIRAPT International Conference on High Pressure Physics, Amsterdam, 1985 [*Physica* **139&140B**, 491 (1986)].
²³L. Camphausen, G. A. N. Connel, and W. Paul, *Phys. Rev. Lett.* **26**, 184 (1971).
²⁴E. Mendez, C. A. Chang, H. Takaoka, L. L. Chang, and L. Esaki, *J. Vac. Sci. Technol.* **1**, 152 (1983).
²⁵M. Naganuma, Y. Susuki, and H. Okamoto, *Appl. Phys. Lett.* **40**, 983 (1982).
²⁶P. Lawaetz, *Phys. Rev. B* **4**, 3460 (1971).
²⁷P. Voisin, C. Delalande, M. Voos, L. L. Chang, A. Segmuller, C. A. Chang, and L. Esaki, *Phys. Rev. B* **30**, 2276 (1984).
²⁸T. Tuomi, M. Cardona, and F. M. Pollak, *Phys. Status Solidi* **40**, 227 (1970); L. D. Laude, M. Cardona, and F. M. Pollak, *Phys. Rev. B* **1**, 1436 (1970).
²⁹G. Martinez, in *Optical Properties of Solids*, edited by M. Balkanski (North-Holland, Amsterdam, 1980), p. 194.
³⁰U. Venkateswaran, M. Chandrasekhar, H. R. Chandrasekhar, B. A. Vojak, F. A. Chambers, and J. M. Meese, *Phys. Rev. B* **33**, 8416 (1986).
³¹J. P. Leburton and K. Kahen, *Superlattices Microstructures* **1**, 49 (1985).